19th Brazilian Congress of Thermal Sciences and Engineering
November 6th–10th, 2022, Bento Gonçalves - RS - Brazil

ENC-2022-0316
INFLUENCE ANALYSIS OF THE CLOSING PARAMETERS IN THE UNIT CELL MODEL FOR GAS-LIQUID FLOWS IN THE INTERMITTENT PATTERN

Alysson Henrique Rublesperger de Almeida*
Victor Vaurek Dimbarre†
Luiz Eduardo Melo Lima‡
Department of Mechanics, Federal University of Technology—Paraná—, Ponta Grossa, PR 84017-220, Brazil
*alysson.2018@alunos.utfpr.edu.br, †victordimbarre@alunos.utfpr.edu.br, ‡lelima@utfpr.edu.br

Abstract. *A succession of liquid pistons (aerated or non-aerated) and elongated gas bubbles parallel with a thin liquid film that repeats itself over the pipe in a non-periodic way describes the intermittent or slug flow. These flows can occur in a steady state considering the unit cell concept. Thus, the hydrodynamic parameters of this kind of flow can be estimated using several models developed based on this concept. In closing these models, several empirical correlations help predict essential parameters, which depend on the primary characteristics of the flow and the pipe. In this context, this work aims to numerically analyze the performance of one of these more complete models, considering several correlations, both for unit cell frequency and slug liquid holdup. A computational code written in MATLAB gave the solution of the unit cell model with various empirical correlations to estimate the closure parameters in this work. The governing equation of the model was solved using the finite difference method. The numerical results for the pressure gradient were compared with experimental data from the literature to demonstrate which combinations of correlations were more satisfactory, validating the model implemented computationally.*

Keywords: *two-phase flow, slug flow, modeling, numerical analysis.*

1. INTRODUCTION

Multiphase flow is present in nature in various situations, such as rain, snow, tornadoes, typhoons, and air and water pollution. Furthermore, this phenomenon occurs in many processes, for example, combustion in engines, propulsion systems, fluids in the human body, nuclear power generation, oil and gas transportation, and food production, among others (Kolev, 2005). Thereby, methods to predict its behavior are necessary. Among the possible configurations that multiphase flow can present, three main patterns stand out when a gas-liquid mixture occurs: dispersed, separated, and intermittent. These patterns arise depending on the characteristics of the phases involved and their physical properties, the pipe geometrical properties (diameter, inclination, and roughness), and initial operating conditions, such as the flow rates of each phase. Among these configurations, the intermittent gas-liquid flow (slug flow) is present in several processes, as it occurs in a wide interval of gas and liquid flow rates. Therefore, there is a great effort to develop an adequate physical model that accurately represents its behavior, despite the dependence on empirical correlations (Shoham, 2006).

Intermittent flow (pattern) is characterized by liquid pistons (slugs), with or without dispersed gas bubbles (depending on operating conditions), followed by elongated gas bubbles containing a well-defined contact interface with a liquid film. Along the pipe, there is a repetition of this structure resulting from this pattern. Wallis (1969) suggested an approach in which the intermittent flow regions constitute two distinct patterns: dispersed flow for the liquid slug and separate flow for the elongated gas bubble. Thus, the unit cell concept arises, assuming that this structure occurs as a phenomenon in a steady state, which repeats periodically along the pipe, which resulted in the development of mathematical models that allowed a better understanding of the dynamics in intermittent flow and its relevant parameters.

Dukler and Hubbard (1975) developed the first of these models, considering the flow to be one-dimensional and with negligible pressure drop along the elongated bubble length. Furthermore, the mass and *momentum* balances do not consider the gas phase influences. In this way, a free surface serves as a model for the film in the elongated bubble region.

Later, Gregory *et al.* (1978) recognized the need for a term that considered the elongated bubble drift velocity relative to the film. This velocity greatly influences the model, making evident the hydrodynamic differences when compared to an

elongated bubble moving in stagnant liquid, especially in relatively wide pipes with slight inclinations. In addition, they related the velocity of the elongated bubble nose with the mixture superficial velocity.

Kokal and Stanislav (1989) found the dependence of pressure drop on flow patterns. They presented an unprecedented model that considers the shear stress at the interface between an elongated bubble and its film. However, they did not regard the shear stress of the elongated bubble with the pipe wall. Their results showed satisfactory agreement with experimental data, mainly for higher gas flows, when compared to previous models, which did not consider the influence of interfacial shear stress.

These models had a remarkable evolution in the work of Taitel and Barnea (1990), which still stands today as a reference in obtaining results for intermittent flow. Their model considers the most complete, serving as a basis for improvements proposed over the years since then; because, for the first time, the model considers the effects of the gas phase. These effects are present both in the elongated bubble, taking into account the shear stress of the bubble with the pipe wall, and in the liquid slug, where there may be the presence of small dispersed bubbles that interact with the liquid phase, presenting velocity different from the same.

Seeking to improve the Taitel and Barnea (1990) model and the closure correlations, Andreussi *et al.* (1993) highlighted that the presence of dispersed bubbles in the film is significant for air-water flows at high velocities and, possibly, more expressive for liquids with low surface tension. This phenomenon may be relevant in determining the average fraction of liquid present in a unit cell. Thus, they considered the presence of two distinct gas streams in their model, in the elongated bubble and another dispersed in the film.

Cook and Behnia (1997) concluded in their work that the accuracy of the results, based on the model of Taitel and Barnea (1990), significantly influences the choice of correlation for calculating the translational velocity of the elongated bubble. Considering this velocity is around 1.2 times the value of the mixture's superficial velocity, it becomes possible to obtain more consistent results. Furthermore, their model disregarded gravity's influence on the gas phase. They analyzed the pressure gradient separately for each phase so that the terms related to the buoyant force are functions of gas and liquid densities.

Fagundes Netto *et al.* (1999) significantly contributed to a better understanding of the structure of intermittent flow and its development along the pipe. Analyzing the influence of the flow velocity and the bubble volume on its shape achieved this contribution. They also proposed a model that considers the elongated bubble to consist of four parts: the nose, the body, the tail, and a hydraulic jump between the tail and the body. This hydraulic jump represents a rapid change in film thickness, causing a static pressure difference.

Cook and Behnia (2000) proposed a reformulation of the Taitel and Barnea (1990) model, adding a term due to the effective viscosity of the aerated liquid slug in the pressure drop calculation. Orell (2005) found in their experimental study that this term is significant for high superficial velocities of the gas phase, especially for air-oil systems.

In that context, the present work aims to compare the results obtained with the Taitel and Barnea (1990) model against experimental data from the literature, considering different combinations of empirical correlations to close the model, also from literature. A computational code developed in MATLAB® in the present work performs the numerical integration of the model and the calculation of empirical correlations and auxiliary variables to determine which combination of correlations provides the most satisfactory results.

2. MODEL

This section shows the physical modeling using the unit cell model proposed by Taitel and Barnea (1990), based on the description given by Shoham (2006). Additionally, the model calculations need the introduction of the variables and closing correlations. Considering an isothermal gas-liquid mixture (with known physical properties of the phases: density ρ, dynamic viscosity μ, and surface tension σ) flowing with volumetric flow rate Q in a pipe of length L, diameter D, perimeter S, area A, and inclination θ, the unit cell has a length L_U, resulting from the sum of L_F and L_S, which represent the lengths of the film and the slug, respectively, according to Fig. 1.

Taitel and Barnea (1990) sought to unify a model applicable to flows in pipes with any inclination, proposing three approaches to studying film hydrodynamics, two of which assume simplifying hypotheses. The first takes an equilibrium and constant film thickness along the region of the elongated bubble and the film: $h_F \equiv h_{Fe} = \text{constant}$ and $-(\mathrm{d}p/\mathrm{d}z) \neq 0$. The second assumes a free surface open-channel flow for the film: $h_F \neq \text{constant}$ and $-(\mathrm{d}p/\mathrm{d}z) = 0$. The third presents a more precise description that requires the numerical solution of a more detailed equation to estimate the film profile, with $h_F \neq \text{constant}$ and $-(\mathrm{d}p/\mathrm{d}z) \neq 0$, being the approach used in the present work and defined by:

$$\frac{\mathrm{d}h_F}{\mathrm{d}z_F} = \frac{\frac{\tau_F S_F}{A_F} - \frac{\tau_G S_G}{A_G} - \tau_I S_I \left(\frac{1}{A_F} + \frac{1}{A_G}\right) + (\rho_L - \rho_G)\, g \sin\theta}{(\rho_L - \rho_G)\, g \cos\theta - \left[\rho_L \frac{(V_{TB} - V_{LTB})^2}{H_{LTB}} + \rho_G \frac{(V_{TB} - V_{GTB})^2}{1 - H_{LTB}}\right] \frac{S_I}{A}} \tag{1}$$

Section 2.1 presents the numerical integration procedure of Eq. (1) to obtain the length of the film L_F (or the elongated bubble). This procedure ends when the liquid phase mass balance is satisfied, which depends on the unit cell frequency υ ($\equiv V_{TB}/L_U$), estimated by empirical correlations (some of which are discussed in Section 2.2), according to:

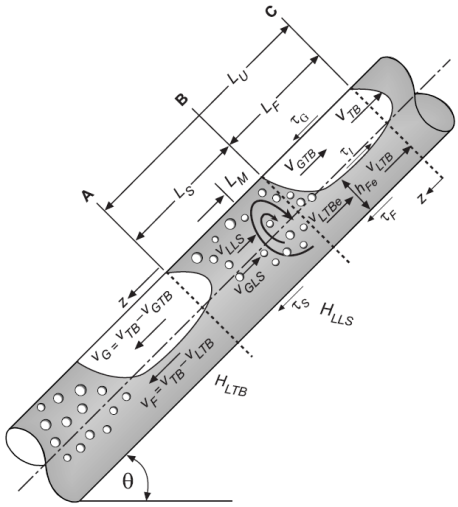

Figure 1. Representation of the model and its variables (Shoham, 2006).

$$V_{SL} = V_{LLS} H_{LLS} + \upsilon \left[(1 - H_{LLS})\, L_F - \int_0^{L_F} (1 - H_{LTB})\, \mathrm{d}z_F \right] \tag{2}$$

where the liquid superficial velocity is V_{SL} ($\equiv Q_L/A$), just as the gas superficial velocity is V_{SG} ($\equiv Q_G/A$).

The shear stresses of the phases with the pipe walls (τ_F and τ_G) must be expressed using the local velocities of the phases (V_{LTB} and V_{GTB}):

$$\tau_F = \frac{1}{2} f_F \rho_L |V_{LTB}| V_{LTB} \tag{3}$$

$$\tau_G = \frac{1}{2} f_G \rho_G |V_{GTB}| V_{GTB} \tag{4}$$

On the other hand, the interfacial shear stress τ_I considers the relative velocity between the phases:

$$\tau_I = \frac{1}{2} f_I \rho_G |V_{GTB} - V_{LTB}| \left(V_{GTB} - V_{LTB}\right) \tag{5}$$

The friction factors (Fanning) of the phases (f_F and f_G) can be determined using the Blasius correlation for hydraulically smooth pipes:

$$f_F = C \left(\frac{V_{LTB} D_F \rho_L}{\mu_L} \right)^{-n} \tag{6}$$

$$f_G = C \left(\frac{V_{GTB} D_G \rho_G}{\mu_G} \right)^{-n} \tag{7}$$

with $C = 16$ and $n = 1$ if laminar and $C = 0.046$ and $n = 0.2$ if turbulent; for rough pipes, there are several other correlations in the literature for this.

Depending on the interface shape, the interfacial friction factor f_I can be estimated as a function of the dimensional film thickness δ_F ($\equiv h_F/D$):

$$f_I = \begin{cases} 0.014 & \text{if a flat film (Cohen and Hanratty, 1968; Shoham and Taitel, 1984)} \\ 0.005\,(1 + 300\delta_F) & \text{if a concentric film (Wallis, 1969)} \end{cases} \tag{8}$$

The kinematic law proposed by Nicklin (1962) adequately models the translational velocities of the elongated bubble V_{TB} and the bubbles dispersed in the liquid slug V_{GLS} as a function of the mixture superficial velocity V_M ($\equiv V_{SL} + V_{SG}$):

$$V_{TB} = C_{0TB} V_M + V_{\infty TB} \equiv C_{0TB} V_M + \mathrm{Fr}_{\infty TB} \sqrt{gD\,(1 - \rho_G/\rho_L)} \tag{9}$$

$$V_{GLS} = C_{0GLS} V_M + V_{\infty GLS} \equiv C_{0GLS} V_M + \mathrm{Fr}_{\infty GLS} \sqrt{gD\,(1 - \rho_G/\rho_L)} \tag{10}$$

Table 1 presents the definitions for the distribution parameters, C_{0TB} and C_{0GLS}, and the drift Froude numbers, $\mathrm{Fr}_{\infty TB}$ and $\mathrm{Fr}_{\infty GLS}$, of the elongated bubble (Bendiksen, 1984; Weber, 1981) and the dispersed bubbles (Harmathy, 1960), presented in Eqs. (9) and (10), as a function of the Eötvös and Froude numbers for the mixture, defined as $\mathrm{Eo} = gD^2(\rho_L - \rho_G)/\sigma$ and $\mathrm{Fr} = V_M/\sqrt{gD(1 - \rho_G/\rho_L)}$, respectively.

Table 1. Definitions of distribution parameters and drift Froude numbers considering turbulent flow (Lima, 2011).

Bubble(s)	k	C_{0k}	$\mathrm{Fr}_{\infty k}$	Criterion
Elongated	TB	$1 + 0.2\sin^2\theta$	$\left(0.542 - \frac{1.76}{\mathrm{Eo}^{0.56}}\right)\cos\theta + \frac{0.345\sin\theta}{\left(1+3805\mathrm{Eo}^{-3.06}\right)^{0.58}}$	$\mathrm{Fr} < 3.5$
		1.2	$\frac{0.345\sin\theta}{\left(1+3805\mathrm{Eo}^{-3.06}\right)^{0.58}}$	$\mathrm{Fr} \geq 3.5$
Dispersed	GLS	$1 + 0.2\sin^2\theta$	$1.54\mathrm{Eo}^{-1/4}H_{LLS}^{7/4}\sin\theta$	–

Mass balances and definitions of relative velocities provide expressions for the average velocities of liquid in the slug (V_{LLS}), film (V_{LTB}), and gas in the elongated bubble (V_{GTB}):

$$V_{LLS} = \frac{V_M - V_{GLS}\left(1 - H_{LLS}\right)}{H_{LLS}} \tag{11}$$

$$V_{LTB} = V_{TB} - \frac{\left(V_{TB} - V_{LLS}\right)H_{LLS}}{H_{LTB}} \tag{12}$$

$$V_{GTB} = \frac{V_M - V_{LTB}H_{LTB}}{1 - H_{LTB}} \tag{13}$$

Where H_{LLS} is the slug liquid holdup (fraction), often estimated by empirical correlations from the literature (some of which are discussed in Section 2.3). H_{LTB} is the holdup of film or liquid in the elongated bubble region, defined from the geometrical relations of the interfaces, as well as perimeters S_k, areas A_k, and hydraulic diameters D_k of the phases or regions k $(= G, F, I)$, according to Tab. 2.

Table 2. Geometrical properties of interfaces (Lima, 2011).

Geometrical	Interface	
properties	Flat	Concentric
S_G	$D\left(\pi - \lambda_F/2\right)$	0
S_F	$D\lambda_F/2$	πD
S_I	$D\sin\left(\lambda_F/2\right)$	$\pi D\left(1 - 2\delta_F\right)$
A_G	$D^2\left(2\pi - \lambda_F + \sin\lambda_F\right)/8$	$\pi D^2\left(1 - 2\delta_F\right)^2/4$
A_F	$D^2\left(\lambda_F - \sin\lambda_F\right)/8$	$\pi D^2\delta_F\left(1 - \delta_F\right)$
D_G	$D\left[1 + \frac{\sin(\lambda_F/2) - \sin\lambda_F/2}{2(2\pi - \lambda_F + \sin\lambda_F)}\right]^{-1}$	$D\left(1 - 2\delta_F\right)$
D_F	$D\left(1 - \sin\lambda_F/\lambda_F\right)$	$D\left[4\delta_F\left(1 - \delta_F\right)\right]$
H_{LTB}	$\left(\lambda_F - \sin\lambda_F\right)/\left(2\pi\right)$	$4\delta_F\left(1 - \delta_F\right)$

The geometrical properties shown in Tab. 2 are functions of the angle resulting from the flat interface, defined as $\lambda_F = 2\arccos(1 - 2\delta_F)$, or directly in terms of the dimensionless film thickness δ_F, for a concentric interface.

2.1 Numerical solution procedure

Having all the variables necessary to calculate Eq. (1), it is possible to start the process of obtaining the bubble profile, an essential variable in determining relevant parameters for intermittent gas-liquid flows such as the pressure drop and transfer rates of mass and heat. All terms of Eq. (1) vary with the axial coordinate z_F. However, the physical properties of the fluids and the pipe characteristics are constant at each step of numerical integration, as are the unit cell frequency and the slug liquid holdup (both estimated by empirical correlations).

The numerical integration of Eq. (1) to obtain the profile of the elongated bubble, $h_F = h_F(z_F)$, was performed using the fourth-order Runge–Kutta method. This numerical method, the model equation, the auxiliary equations, and the empirical correlations are implemented in a computational code developed in MATLAB®. Starting the integration at the nose of the bubble and marching along its length until Eq. (2) is satisfied. An essential element is the evaluation of the initial film thickness, which Shoham (2006) suggests the use of $h_F(z_F = 0) = H_{LLS}D$. That is, the starting point, at the nose of the elongated bubble, is obtained considering the liquid holdup in this coordinate is equal to the average slug liquid holdup since this coordinate is at the interface of the analyzed cell and the last cell.

However, depending on the input data of the problem, it may result in a wrong solution. In the region of the bubble nose, there may be an inflection point in the profile, according to Fig. 1. Thus, if the initial estimate is above this inflection point, the derivative shown in Eq. (1) becomes positive. The integration will occur in the "upper" part of the inflection point. Therefore, before starting the march of integration along the elongated bubble, the derivative defined in Eq. (1) is

negative. Thus, after the initial estimate, if Eq. (1) is negative, the integration process begins; otherwise, assuming that $h_F = h_F(z_F = 0)$ is above the inflection point, this initial thickness decreases using a suitable step size until the derivative defined in Eq. (1) becomes negative.

Another critical detail concerns the integration step size used in the bubble nose and body. The slope is much greater in the nose than in the body. Especially near the starting point, where $(\mathrm{d}h_F/\mathrm{d}z) \to \infty$ due to inflection. Thus, one solution is to use a smaller step for the nose region and, as Eq. (1) results in relatively smaller values, gradually increase the step size to obtain a detailed nose profile. This solution avoids an excessive number of steps in the body region, which tends to be almost horizontal, i.e. $(\mathrm{d}h_F/\mathrm{d}z) \to 0$.

2.2 Cell frequency correlations

Carvalho and Lima (2018) analyzed the accuracy of various empirical correlations against experimental data of unit cell frequency υ. Five υ correlations that presented the best results are shown in Tab. 3 and used to analyze the performance of the unit cell model in the present study, in combination with correlations for slug liquid holdup H_{LLS} presented in the next section.

Table 3. Definitions of the cell frequency correlations analyzed in this study.

Correlation	Author	υ / [Hz]
CFC1	Gregory and Scott (1969)	$0.0226\left[\phi_L\left(\frac{19.75}{gD}+\mathrm{Fr}^2\right)\right]^{6/5}$
CFC2	Jepson and Taylor (1993)	$\phi_L\left(\frac{4.76\times10^{-3}V_M^2+0.035V_M}{D}\right)$
CFC3	Shell (Zabaras, 1999)	$\sqrt{\frac{g}{D}}\left\{0.048\mathrm{Fr}_L^{0.81}+0.73\mathrm{Fr}_L^{2.34}\left[(\mathrm{Fr}_G+\mathrm{Fr}_L)^{0.1}-1.17\mathrm{Fr}_L^{0.064}\right]^2\right\}$
CFC4	Fossa *et al.* (2003)	$\frac{V_{SG}}{D}\left(\frac{0.044\phi_L}{1-1.71\phi_L+0.70\phi_L^2}\right)$
CFC5	Wang *et al.* (2007)	$\frac{V_{SG}}{D}\left(\frac{0.05\phi_L}{1-1.675\phi_L+0.768\phi_L^2}\right)$

In Table 3, ϕ_L $(= V_{SL}/V_M)$ is the homogeneous liquid holdup, Fr_G $(= V_{SG}/\sqrt{gD})$ is the gas Froude number, and Fr_L $(= V_{SL}/\sqrt{gD})$ is the liquid Froude number.

2.3 Liquid holdup correlations

Barboza *et al.* (2020) analyzed the accuracy of various empirical correlations against experimental data of slug liquid holdup H_{LLS}. Five H_{LLS} correlations that presented the best results are shown in Tab. 4 and used to analyze the performance of the unit cell model in the present study, in combination with correlations for unit cell frequency υ presented in the previous section.

Table 4. Definitions of the liquid holdup correlations analyzed in this study.

Correlation	Author	H_{LLS}
LHC1	Gregory *et al.* (1978)	$\left[1+(V_M/8.66)^{1.39}\right]^{-1}$
LHC2	Malnes (1982)	$1-\left[1+\frac{83}{\mathrm{Fr}}\left(\frac{1-\rho_G/\rho_L}{\mathrm{Eo}}\right)^{1/4}\right]^{-1}$
LHC3	Ferschneider (1983)	$\left[1+\mathrm{Eo}^{0.2}\widehat{\mathrm{Fr}}^{\,2}/50\right]^{-2}$
LHC4	Xu (2013)	$\left[1+(V_M/9.514)^{1.274}\right]^{-1}$
LHC5	Al-Ruhaimani *et al.* (2018)	$\frac{0.266}{\widehat{\mathrm{Fr}}\sqrt{\mathrm{N}_\mu}}+0.912$

In Table 4, $\widehat{\mathrm{Fr}}$ $(= \mathrm{Fr}/\sqrt{1-\rho_G/\rho_L})$ is the modified Froude number, and N_μ $(= \sqrt{gD^3\rho_L(\rho_L-\rho_G)}/\mu_L)$ is the inverse viscosity number.

3. ANALYSIS METHOD

The accuracy analysis of the correlations combinations employed in the unit cell model is based on the determination of the relative deviation modulus mean value ϵ_R between the calculated (calc.) and measured (meas.) values for the dimensionless film length L_F/D. Also, this analysis considers the RMS (Root Mean Square) values of the relative deviations referring to the N experimental tests described in Section 3.1. The values of ϵ_R and RMS are calculated by:

$$\epsilon_R = \frac{1}{N} \sum \frac{|(L_F/D)_{calc.} - (L_F/D)_{meas.}|}{(L_F/D)_{meas.}} \tag{14}$$

$$\text{RMS} = \sqrt{\frac{1}{N} \sum \left[\frac{(L_F/D)_{calc.} - (L_F/D)_{meas.}}{(L_F/D)_{meas.}} \right]^2} \tag{15}$$

3.1 Experimental data

For the influence analysis of the closing parameters in the unit cell model, the experimental data used in this work comes from other work found in the literature. Bueno (2010) conducted ten experiments using air and water as a mixture in a horizontal test section of $306D$ length and 26 mm inner diameter. The experimental apparatus consists of the flow in two separate air and water circuits. These circuits are carried to a mixer to constitute the two-phase flow, which in the sequence passes through the acrylic test section, where two different stations measure the data, one $77D$ and another $257D$, downstream of the mixer. At these stations, impedance sensors monitor the intermittent flow data, and a data acquisition system obtains and processes the data. After going through the test section, a vertical pipe of 75 mm inner diameter acts as an air and water separator for the mixture discharged into this pipe. Tab. 5 presents the parameters set or measured in the experimental tests by Bueno (2010).

Table 5. Values of parameters set or measured in the experimental tests performed by Bueno (2010).

Test	V_{SG} / (cm/s)	V_{SL} / (cm/s)	V_{SG}/V_{SL}	ϕ_L	P / (mbar)	L_F/D
1	142.1	29.0	4.90	0.17	1009	140.2
2	84.8	29.0	2.92	0.25	982	67.5
3	59.0	31.0	1.90	0.34	983	40.5
4	112.2	60.0	1.87	0.35	1012	34.8
5	185.9	121.0	1.54	0.39	1058	34.1
6	60.1	61.0	0.99	0.50	991	15.7
7	111.7	120.0	0.93	0.52	1031	16.0
8	82.7	92.0	0.90	0.53	1007	13.9
9	30.2	60.0	0.50	0.66	992	7.5
10	56.4	120.0	0.47	0.68	1018	7.8

The fluids properties necessary for the numerical integration of the unit cell model come from literature, considering the operational conditions of the Bueno (2010) experiments: atmospheric pressure of $P_{atm} = 947$ mbar and ambient temperature $T = 25$ °C. The ideal gas state equation estimates the air density, considering this ambient temperature and the local absolute pressure at each experimental test.

4. RESULTS AND DISCUSSION

Tables 6 and 7 show the relative deviation modulus mean values ϵ_R and its RMS values, respectively, for the dimensionless film length L_F/D. These deviations correspond to the L_F/D calculated values by the unit cell model for all combinations of the correlations analyzed, compared with the Bueno (2010) experimental dataset for L_F/D. The lines and columns in Tabs. 6 and 7 represent correlations employed for the cell frequency and liquid holdup, according to Tabs. 3 and 4, respectively.

Table 6. Relative deviation modulus mean values for the dimensionless film length.

	LFC1	LFC2	LFC3	LFC4	LFC5
CFC1	19.86	20.86	18.45	20.05	23.09
CFC2	44.85	41.81	46.33	43.86	44.58
CFC3	22.32	21.20	22.28	21.99	22.34
CFC4	9.32	9.55	9.95	9.07	9.14
CFC5	12.74	12.67	13.08	12.75	11.11

The worst combination of correlations corresponds to CFC2 (Jepson and Taylor, 1993) and LHC3 (Ferschneider, 1983). The minimal value of ϵ_R was for CFC4 (Fossa *et al.*, 2003) with LHC4 (Xu, 2013) (Tab. 6). The minimal value of RMS was for CFC4 (Fossa *et al.*, 2003) with LHC5 (Al-Ruhaimani *et al.*, 2018) (Tab. 7). However, all correlations of liquid holdup produce small values of standard deviation in ϵ_R ($\leq 1.70\%$) and RMS ($\leq 2.72\%$) for each correlation of cell

Table 7. RMS values of the relative deviation for the dimensionless film length.

	LFC1	LFC2	LFC3	LFC4	LFC5
CFC1	23.19	24.07	22.04	23.38	26.41
CFC2	53.96	50.11	56.78	52.88	50.56
CFC3	24.99	23.20	25.66	24.37	25.02
CFC4	13.82	14.74	13.91	14.08	13.34
CFC5	15.41	15.76	15.96	15.56	13.85

frequency. On the other hand, all correlations of cell frequency produce significant values of standard deviation in ϵ_R ($\leq 14.40\%$) and RMS ($\leq 17.37\%$) for each correlation of liquid holdup. This result means that the model is more sensitive to the influence of the cell frequency than the influence of the liquid holdup, at least in determining the film length.

Figure 2 shows the profiles of the dimensionless liquid thickness h_F/D as a function of the non-dimensional axial coordinate z_F/D for each test condition of the Bueno (2010) experimental dataset, considering the combination of CFC4 (Fossa *et al.*, 2003) with LHC4 (Xu, 2013). Each profile in Fig. 2 corresponds to a homogeneous liquid holdup ϕ_L of all the tests of the Bueno (2010) experimental dataset. Being five tests with $\phi_L < 0.5$ (Fig. 2a) and five tests with $\phi_L \geq 0.5$ (Fig. 2b). These ϕ_L values are the result of distinct combinations of gas and liquid superficial velocity values.

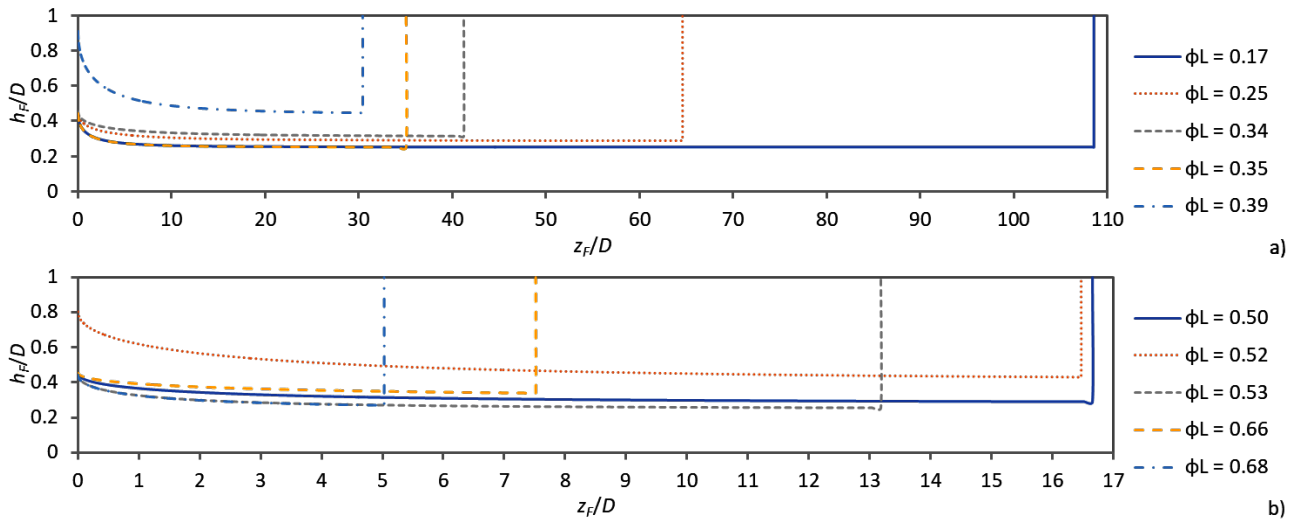

Figure 2. Profiles of the dimensionless liquid thickness as a function of the dimensionless axial coordinate: a) $\phi_L < 0.5$; b) $\phi_L \geq 0.5$.

Figure 2 demonstrates that the dimensionless film length L_F/D decreases with the increase of the homogeneous liquid holdup ϕ_L, as expected from both theory and literature. Also, the dimensionless film thickness h_F/D that defines the film profile strongly depends on the gas-liquid ratio J_G/J_L and ϕ_L, as seen in Tab. 5.

Furthermore, the problem of model integration in the bubble nose region, described in Section 2.1, is highlighted, which results in relatively small initial film thicknesses depending on the gas-liquid ratio, which also influences the film length and thickness along the bubble body.

5. CONCLUSIONS

This work presents an influence analysis of the closing parameters in the unit cell model for gas-liquid flows in the intermittent pattern. The closing parameters analyzed are the unit cell frequency and slug liquid holdup, considering the usage of five distinct correlations from the literature for each parameter in the model. The best combination of correlations found in this analysis was Fossa *et al.* (2003) correlation for the cell frequency with Xu (2013) or Al-Ruhaimani *et al.* (2018) correlation for the liquid holdup. The results from the unit cell model integration demonstrate that the cell frequency influences the model more significantly than the liquid holdup. The present analysis verified the dependence of the length and thickness of the liquid film with the homogenous liquid holdup and gas-liquid ratio, demonstrating that the model results agree with both theory and literature. Future works can improve the model integration process to allow the integration of the bubble nose region with better precision and analyses of other closing parameters in the model.

6. ACKNOWLEDGEMENTS

This study was financed in part by the Fundação Araucária — Brasil (UTFPR/PROPPG n.º 02/2021). The authors also thank the Federal University of Technology—Paraná.

7. REFERENCES

Al-Ruhaimani, F., Pereyra, E., Sarica, C., Al-Safran, E. and Torres, C., 2018. "Prediction of slug-liquid holdup for high-viscosity oils in upward gas/liquid vertical-pipe flow". *SPE Production & Operations*, Vol. 33, No. 2, pp. 281–299. DOI 10.2118/187957-PA.

Andreussi, P., Bendiksen, K.H. and Nydal, O.J., 1993. "Void distribution in slug flow". *Int. J. Multiph. Flow*, Vol. 19, No. 5, pp. 817–828. DOI 10.1016/0301-9322(93)90045-v.

Barboza, G.F., Machado, P.L.O. and Lima, L.E.M., 2020. "Correlations review for the slug liquid holdup prediction in intermittent gas-liquid flows". In *Proceedings of the 18th Brazilian Congress of Thermal Sciences and Engineering (ENCIT)*. Brazilian Association of Engineering and Mechanical Sciences (ABCM), Rio de Janeiro, RJ, Brazil, pp. 346:1–346:9. DOI 10.26678/ABCM.ENCIT2020.CIT20-0346.

Bendiksen, K.H., 1984. "An experimental investigation of the motion of long bubbles in inclined tubes". *Int. J. Multiph. Flow*, Vol. 10, No. 4, pp. 467–483. DOI 10.1016/0301-9322(84)90057-0.

Bueno, L.G.G., 2010. *Estudo experimental de escoamentos líquido-gás intermitentes em tubulações inclinadas [Experimental analysis of slug flow in inclined lines]*. Master's thesis, Faculty of Mechanical Engineering (FEM), State University of Campinas (Unicamp), Campinas, SP, Brazil. DOI 10.47749/T/UNICAMP.2010.771387. URL https://hdl.handle.net/20.500.12733/1612461.

Carvalho, G.L. and Lima, L.E.M., 2018. "A review of frequency correlations for the intermittent gas-liquid flow in horizontal pipes". In *Proceedings of the 17th Brazilian Congress of Thermal Sciences and Engineering (ENCIT)*. Brazilian Association of Engineering and Mechanical Sciences (ABCM), Rio de Janeiro, RJ, Brazil, pp. 251:1–251:10. DOI 10.26678/ABCM.ENCIT2018.CIT18-0251.

Cohen, L.S. and Hanratty, T.J., 1968. "Effect of waves at a gas—liquid interface on a turbulent air flow". *J. Fluid Mech.*, Vol. 31, No. 3, pp. 467–479. DOI 10.1017/S0022112068000285.

Cook, M. and Behnia, M., 1997. "Film profiles behind liquid slugs in gas-liquid pipe flow". *AIChE J.*, Vol. 43, No. 9, pp. 2180–2186. DOI 10.1002/aic.690430904.

Cook, M. and Behnia, M., 2000. "Pressure drop calculation and modelling of inclined intermittent gas–liquid flow". *Chem. Eng. Sci.*, Vol. 55, No. 20, pp. 4699–4708. DOI 10.1016/S0009-2509(00)00065-8.

Dukler, A.E. and Hubbard, M.G., 1975. "A model for gas-liquid slug flow in horizontal and near horizontal tubes". *Ind. Eng. Chem. Fundam.*, Vol. 14, No. 4, pp. 337–347. DOI 10.1021/i160056a011.

Fagundes Netto, J.R., Fabre, J. and Peresson, L., 1999. "Shape of long bubbles in horizontal slug flow". *Int. J. Multiph. Flow*, Vol. 25, No. 6-7, pp. 1129–1160. DOI 10.1016/s0301-9322(99)00041-5.

Ferschneider, G., 1983. "Ecoulements diphasiques gaz-liquide à poches et à bouchons en conduites". *Revue de l'Institut Français du Pétrole*, Vol. 38, No. 2, pp. 153–182. DOI 10.2516/ogst:1983010.

Fossa, M., Guglielmini, G. and Marchitto, A., 2003. "Intermittent flow parameters from void fraction analysis". *Flow Meas. Instrum.*, Vol. 14, No. 4, pp. 161–168. DOI 10.1016/s0955-5986(03)00021-9.

Gregory, G.A., Nicholson, M.K. and Aziz, K., 1978. "Correlation of the liquid volume fraction in the slug for horizontal gas-liquid slug flow". *Int. J. Multiph. Flow*, Vol. 4, No. 1, pp. 33–39. DOI 10.1016/0301-9322(78)90023-x.

Gregory, G.A. and Scott, D.S., 1969. "Correlation of liquid slug velocity and frequency in horizontal cocurrent gas-liquid slug flow". *AIChE J.*, Vol. 15, No. 6, pp. 933–935. DOI 10.1002/aic.690150623.

Harmathy, T.Z., 1960. "Velocity of large drops and bubbles in media of infinite or restricted extent". *AIChE J.*, Vol. 6, No. 2, pp. 281–288. DOI 10.1002/aic.690060222.

Jepson, W.P. and Taylor, R.E., 1993. "Slug flow and its transitions in large-diameter horizontal pipes". *Int. J. Multiph. Flow*, Vol. 19, No. 3, pp. 411–420. DOI 10.1016/0301-9322(93)90057-2.

Kokal, S.L. and Stanislav, J.F., 1989. "An experimental study of two-phase flow in slightly inclined pipes—II. Liquid holdup and pressure drop". *Chem. Eng. Sci.*, Vol. 44, No. 3, pp. 681–693. DOI 10.1016/0009-2509(89)85043-2.

Kolev, N.I., 2005. *Multiphase flow dynamics*. Springer, Berlin, Germany; New York, NY, USA, 2nd edition.

Lima, L.E.M., 2011. *Análise do modelo de mistura aplicado em escoamentos isotérmicos gás-líquido [Analysis of mixture model applied in gas-liquid isothermals flows]*. Ph.D. thesis, Faculty of Mechanical Engineering (FEM), State University of Campinas (Unicamp), Campinas, SP, Brazil. DOI 10.47749/T/UNICAMP.2011.804225. URL https://hdl.handle.net/20.500.12733/1615845.

Malnes, D., 1982. "Slug flow in vertical, horizontal and inclined pipe". Technical report, Institute for Energy Technology, Kjeller, Norway. Report IFE/KR/E-83/002.

Nicklin, D.J., 1962. "Two-phase bubble flow". *Chem. Eng. Sci.*, Vol. 17, No. 9, pp. 693–702. DOI 10.1016/0009-2509(62)85027-1.

Orell, A., 2005. "Experimental validation of a simple model for gas–liquid slug flow in horizontal pipes". *Chem. Eng. Sci.*, Vol. 60, No. 5, pp. 1371–1381. DOI 10.1016/j.ces.2004.09.082.

Shoham, O., 2006. *Mechanistic modeling of gas-liquid two-phase flow in pipes*. Society of Petroleum Engineers (SPE), Richardson, TX, USA, 1st edition.

Shoham, O. and Taitel, Y., 1984. "Stratified turbulent-turbulent gas-liquid flow in horizontal and inclined pipes". *AIChE J.*, Vol. 30, No. 3, pp. 377–385. DOI 10.1002/aic.690300305.

Taitel, Y. and Barnea, D., 1990. "Two-phase slug flow". In J.P. Hartnett and T.F. Irvine Jr., eds., *Advances in Heat Transfer*, Elsevier, Vol. 20, pp. 83–132. DOI 10.1016/s0065-2717(08)70026-1.

Wallis, G.B., 1969. *One-dimensional two-phase flow*. McGraw-Hill, New York, NY, USA, 1st edition.

Wang, X., Guo, L. and Zhang, X., 2007. "An experimental study of the statistical parameters of gas-liquid two-phase slug flow in horizontal pipeline". *Int. J. Heat Mass Transf.*, Vol. 50, No. 11, pp. 2439–2443. DOI 10.1016/j.ijheatmasstransfer.2006.12.011.

Weber, M.E., 1981. "Drift in intermittent two-phase flow in horizontal pipes". *Can. J. Chem. Eng.*, Vol. 59, No. 3, pp. 398–399. DOI 10.1002/cjce.5450590322.

Xu, J.y., 2013. "A simple correlation for prediction of the liquid slug holdup in gas/non-Newtonian fluids: horizontal to upward inclined flow". *Exp. Therm. Fluid Sci.*, Vol. 44, pp. 893–896. DOI 10.1016/j.expthermflusci.2012.06.017.

Zabaras, G.J., 1999. "Prediction of slug frequency for gas-liquid flows". In *Proceedings of the SPE Annual Technical Conference and Exhibition*. Society of Petroleum Engineers (SPE). DOI 10.2118/56462-MS. Paper Number: SPE-56462-MS.

8. RESPONSIBILITY NOTICE

The authors are solely responsible for the printed material included in this paper.